INSTITUTE OF PLASMA PHYSICS

NAGOYA UNIVERSITY

RESEARCH REPORT

NAGOYA, JAPAN

Production of a Synthesized Plasma

Masayuki Fukao+, Yasumasa Takeda++, Masahiro Yokota++,
Yukio Okamoto*, Yoshinobu Kawai**

IPPJ- 213 January 1975

Further communication about this report is to be sent to the Research Information Center, Institute of Plasma Physics, Nagoya University, Nagoya, JAPAN.

+ Permanent Address: Dept. of Nuclear Engineering, Kyoto University

++ Permanent Address: Dept. of Physics, College of Science and Engineering, Nihon University

* Permanent Address: Central Laboratory, Hitachi Ltd.

** Permanent Address: Research Institute for Appl. Mech. Kyushu University

Abstract

Neutralization of helium ion beam extracted from a stationarily operated duoplasmatron is studied. It was confirmed that the neutralization of ion space charge occured mainly at the deceleration stage of the einzel lens, not in the downstream of the neutralizer. The magnetic field and arc current in the duoplasmatron affected substantially the beam divergence.

The energy spectrum of the extracted ions was measured with an energy analyzing system consisting of a pre-decelerator and an electrostatic energy analyzer with 90° deflection. The energy spectrum of ions in the synthesized plasma was essentially defined by the operating conditions of the ion source; gas pressure, magnetic field and arc current in the arc discharge.

A small difference between the space potential and the potential of the emitter changed the characteristics of the synthesized plasma.

1. INTRODUCTION

An intense ion beam with a relatively low energy diverges by the self-space charge, especially in case of a heavy ion beam. 1, 2) Neutralization of the space charge with electrons is an effective method to avoid the divergence of the beam, which has been used in a mass-separator successfully. 3) In electric propulsion for a space flight, charge neutralization is essential to avoid charge up of a vehicle, otherwise ions as properant cannot be removed away to infinite space. In addition to such a practical use, a neutralized ion beam is an interesting medium suitable for studies of kinetic instability and energy relaxation of particles in a plasma. The medium is called "synthesized plasma" by plasma researchers. A synthesized plasma is produced by mixing ions and electrons generated separately. Accordingly, plasma parameters such as temperature of each component and drift velocity between both components can be varied separately. Moreover a precise measurement of the velocity distribution function of the ions is possible because the ions flow with a drift velocity and the whole ions are analyzed without any disturbance to the plasma.

The equipment described in this paper was constructed for an aim to study stability of an ion beam-plasma medium

and mechanism of energy relaxation of fast ion through an interaction with a plasma, which is impotant for plasma heating by neutral beam injection.

According to the theory of two stream instability, 4, 5, 6) stability criterion is determined by the ratio of electron- to ion temperatures and drift velocity between both components. Roughly speaking, a plasma becomes unstable when the drift velocity between ions and electrons exceeds the thermal velocity of electrons. Energy of ion beam from 1 to 20 keV was dealt with in this experiment. The drift velocity for singly charged helium ions in this energy range corresponds to the thermal velocity of electrons with temperature from 0.1 to 3 eV. Hence this equipment is suitable to an experimental study of the two stream instability in a commonly used laboratory plasma with a few eV in electron temperature. In order to measure the energy spread of fast ions caused by such an interaction, an energy analyzer is required with a better resolution than a few eV. It is not realistic to obtain a few eV of resolution around a mean beam energy of 10 keV by a direct measurement. We have successfully employed a pre-deceleration method in which a fast ion was declerated to some hundreds eV and then differentially analyzed by a usual energy analyzer of electrostatic deflection type. In the next

section, we describe the whole experimental equipment and energy analyzing system. In § 3, ion source and lens system are described. In § 4, results of energy analysis and some discussion about the dependence of ion energy spread on the operating conditions of the ion source are described. In § 5, probe characteristics under the existence of an energitic ion beam and effects of a neutralizer to beam focussing and parameters of a produced synthesized plasma are dealt with.

2. EXPERIMENTAL EQUIPMENT

The schematic figure of the experimental equipment is shown in Fig. 1. An ion beam extracted from an ion source of duoplasmatron type is focussed by a lens system with four electrodes and then neutralized with thermionic electrons from a neutralizer located inside the last electrode of the lens system. The neutralized ion beam, namely the synthesized plasma flows to a drift chamber through an orifice of 15 mm in diameter and into a target of copper disc of 40 mm in diameter. A part of the beam flows through a hole of 5 mm in diameter at the center of the target into an ion energy analyzer. The ion source and the lens system will be described in the next section. The neutralizer consists of two strips of thoriated tungsten ribbon of 0.02 x 0.75 mm^2, 30 mm long and shaped to the figure X. The filaments are heated by direct current up to 7 A. The drift chamber is made of a stainless steel tube of 10 cm in diameter and 100 cm long, and a uniform magnetic field with the intensity up to 2.0 KG is applied over 90 cm long. An orifice is located at an entrance of the uniform region of the magnetic field in order to cut off the halo of the ion beam and to define the boundary of the produced synthesized plasma. It also

forms a barrier of neutral gas flow for differential pumping. Neutral gas from the ion source is evacuated by a 6 inch oil diffusion pump and another 4 inch diffusion pump is used to prepare a low base pressure in the drift chamber by differntial pumping. Typically, when the ion source is operated with operating gas pressure of 0.15 Torr in the arc chamber, the gas pressure is 1.5×10^{-5} Torr at the lens system and lower than 1.0×10^{-5} Torr in the drift chamber. The mean free path for charge transfer collision of He^+ ion with energy from 1 to 10 keV is about 100 m at neutral gas pressure of 1×10^{-5} Torr. Considering the difference between the transit time of the fast ions and the staying time of slow ions produced by the charge transfer collisions, a considerable quantity of slow ions exist in the drift chamber. The beam current is absolutely measured with a calorimetric method in which the temperature rise of cooling water of the target is accurately measured with a thermocouple.

An electrostatic energy analyser with 90° deflection was employed to measure the energy spread of the beam ions. The mean radius of curvature and spacing of the deflection electrodes are 100 mm and 10 mm, respectively. A pair of slits of 1 mm in width are located at the focus points, 53.1 mm from the end planes of the deflection electrodes. Since the resolution

of the electrostatic energy analyzer is, even in an ideal case, given by the ratio of a slit width to the mean radius of curvature of the deflection electrodes, it is impossible to detect the energy spread of a few eV from the mean energy of some 10 keV by directly injecting the beam into the deflector. In order to obtain high resolution, the ions through the target were retarded down to 100 eV in the mean energy by a pre-decelerator. The decelerator was composed of eight plane electrodes, 30 mm in inner diameter, 3 mm in thickness and 7 mm in spacing of adjacent electrodes. A collimating electrode with a knife-edged hole of 5 mm in diameter was placed in front of the decelerating electrodes in order to avoid ion bombardment on the decelerating electrodes. The retarding potential was supplied through a floating battery in series connection with the high voltage power supply for ion acceleration so that energy fluctuation of ions due to A.C. ripple contained in the accelerating voltage could be cancelled out. The electrical connection of the energy analyzer system is shown in Fig. 2. The residual energy of retarded ions was adjusted by the terminal voltage of the battery. The plots of energy spread versus the residual energy of decelerated ions showed that the energy resolution of 1 eV or better could be obtained.

3. ION SOURCE AND LENS SYSTEM

A duoplasmatron ion source used in this experiment is traced in Fig. 3. A barium oxide cathode of 30 mm in diameter was used with a power consumption of 150 W. Operating gas pressure in the arc discharge chamber was normally from 0.1 to 0.15 Torr. Helium gas was used throughout this experiment. The anode and the intermediate electrode were water-cooled. A molybdenum tip was mounted at the center of the anode for stationary operation. The tip has a single hole of 1.0 mm in diameter for ion extraction. A small expansion cup made of iron was attached. Although various expansion cups of cylindrical and conical shape with different opening angles and made of iron and copper were employed, no appreciable change in perviance and beam focussing was observed in contradiction to other reports. 8) Arc current and magnetizing coil current were supplied with SCR- and transistor-controlled constant current power sources, respectively.

The geometrical arrangement and electrical circuitry for measureing the characteristic of the ion source and the lens system are shown in Fig. 4. Currents I_j into each electrode j, contains current due to secondary electrons as

well as incident ions. Secondary electron yield by ion bombardment depends on the ion energy and the potential configuration of the lens changes the distribution of the secondary electron current. However, it was assumed that the contribution of the secondary electron current to total current to each electrode was insensitive to the accelerating voltage and lens potential so far as the polarity of applied potential is not changed.

In the first place ion extraction by a single gap was performed. Ion beam tends to converge as the extraction voltage increases. For a given accelerating voltage there exists an optimum density of the plasma in the expansion cup. Total ion current extracted from the souce increased with the arc current but the beam current into the target is not proportional to the total current. Exceeding the optimum density brings on undersirable change of a plasma boundary in the expansion cup and makes the beam diverge. Both the simple acceleration-deceleration lens and the einzel lens with an accelerating potential were insufficient in beam focusing, and much higher lens voltage than accelerating one was required. The einzel lens with a decelerating potential showed a remarkable lens action, but beam current was sm in low energy region and the back-streaming of electrons fro

the neutralizer heated the middle electrode and brought about undersirable loading on the lens power supply. The combination of the acceleration-deceleration lens and the einzel lens with a decelerating potential was examined. The characteristis is shown in Fig. 5. Although it showed complex behaviors, a fairly high intensity of beam current was obtained over a wide range of beam energy. In this figure, k=1 means that the second electrode which is the middle one of the einzel lens is equipotential with the expansion cup, but the length of the electrode is short in comparison with the diameter and so the potential at the center is lower than at the plasma boundary in the expansion cup. In this system a deep negative potential applied to the third electrode suppressed effectively the backstreaming of electrons and wasteful loading of the high voltage power supply.

4. ION ENERGY ANALYSIS WITHOUT OPERATING THE NEUTRALIZER

In the first place we have investigated the dependence of energy spread ΔE and the most probable energy E_m of an ion beam extracted from the duoplasmatron upon various experimental parameters. Schematic diagram of the energy analyzing system is shown in Fig. 2. The residual energy, E_{res} with which the ions produced in the region equipotential to the anode of the ion source enter into the electrostatic energy analyzer after passing through the pre-decelerator, was typically 110 eV. With this circuitry it was assured by monitoring the collector current of the analyzer on an oscilloscope that the A. C. ripple contained in the accelerating high voltage is perfectly cancelled out.

It was preliminally examined that the energy spread ΔE and the most probable energy E_m were primarily determined by the ion source parameters; arc current I_d, source magnet current I_m and operating gas pressure in the arc chamber P_o. The two measured parameters of the energy spectrum were scarecely affected by lens condition, gas pressure in the drift chamber and intensity of the uniform guiding magnetic field although those affected the absolute value of the collector current. Therefore for

eliminating the effect of the stray magnetic field in the extraction region we did not apply the magnetic field in the drift space. For simplifying the operating condition, all the electrodes of the lens system were commonly grounded.

Typical examples of the energy spectra are shown in Fig. 6 where (a) and (b) show the dependences of energy spectrum upon intensity of the source magnetic field and operating gas pressure in the arc chamber, respectively. Fig. 6 (a) shows that the most probable energy increases appreciably as the energy spectrum have broader shape. This correlation between the most probable energy and half width of the energy spectrum is discussed later in this section. The values of E_m, and ΔE are plotted versus I_d, I_m and P_o in Fig. 7, where E_m is measured on the basis of the accelerating voltage V_{ac} and ΔE denotes the half width. It should be noted that E_m exceeds V_{ac} by nearly 8 eV and the increment corresponds to the increase of energy spread ΔE. Our energy analysis of ions from the duoplasmatron source shows that the energy spectrum usually has a single peak and exceptionally has double humps as shown in Fig. 6 (b) at low arc current, low intensity of the source magnetic field and low operating gas pressure in the arc chamber, typically at I_d=1.0 A, I_m=0.2 A, and P_o=0.04 - 0.08 Torr. The latter profile of the

energy spectrum is similar to that measured by G, Gautherin et al. 10)

The existence of ions with a higher energy than the accelerating potential and the double humps in the spectral shape are explained in connection with the formation of a negative anode fall, that is, a positive potential hill which has been studied by G. Gautherin et al. 10) The formation of the potential hill in front of the anode of the duoplasmatron source is attributable to the negative anode fall of space potential in a low pressure arc discharge. 11) The increase of arc current and/or source magnetic field intensity gives rise to the increase of ionization rate and suppression of the removal of ions by diffusion and recombination on the chamber wall. Therefore ion concentration surpasses electron concentration at a position with strongest magnetic field in the vicinity of the anode, thus forming a local potential hill.

The existence of ions with a higher energy than the acceleration voltage and the correlation between the energy spread and the most probable energy are explained as follows. For convenience of later description the typical axial distribution of plasma space potential in the duoplasmatron arc discharge is depicted in Fig. 8. In case of negative anode fall ions produced at any point between the location P and A

are accelerated toward the extraction electrode immediately after they are produced since the electric field is directed toward the extraction electrode. The increase of I_d and/or I_m raises the height of the potential hill. Hence the increase of height of the potential hill causes the corresponding increase of energy spread of ions produced at the slope of the hill. The fact that the difference between the most probable energy of ions and E_{res} (equivalently the accelerating voltage) is nearly half the energy spread ΔE is consistent with the above explanation.

As shown in Fig. 7 (c), both E_m and ΔE decrease with a rise of operating gas pressure P_o in the arc chamber. This behavior is explained as follows: The mean free path of charge transfer collision for He^+ of several eV is very small and estimated to be typically 1 mm or less at H_e gas pressure of 0.1 Torr. Most of the ions produced in the arc discharge, therefore, would suffer charge transfer collisions with the increased neutral atoms in the vicinity of the anode and the expansion cup when the operating gas pressure is raised. Then, the ions extracted into the lens system are to be produced by the charge transfer collision in the anode hole and the expansion cup. There is no large potential gradient in the region with high neutral density, surrounded by the

anode and expansion cup. Therefore the mean energy of the extracted ions are nearly equal to the acceleration potential and have smaller half width in the energy spectra.

Next we investigated the relationship between the energy spectrum of extracted ions with low frequency oscillation in the arc discharge. Fluctuations in discharge voltage of the arc was observed with a spectrum analyzer. The maximum amplitude of the oscillation and the corresponding frequency are plotted versus operating gas pressure P_o in Fig. 9. The low frequency oscillation in the arc discharge was detected only at low operating pressure lower than 0.08 Torr, and did not appear at normal operating pressure P_o=0.15 Torr. Therefore we cannot attribute the above behavior of the ion energy spectrum to the low frequency oscillation in the arc discharge in contradiction to the result reported by Orsay group. 12)

EFFECTS OF NEUTRALIZER AND PRODUCED SYNTHESIZED PLASMA

Synthesized plasma is produced by attaching thermionic electrons from a neutralizer. Plasma parameters such as electron density n_e, electron temperature T_e and space potential V_S were measured by a Langmuir probe. A produced synthesized plasma consists of fast ions, attached thermionic electrons and slow ions which are produced through charge exchange between fast ions and residual neutral atoms. In probe measurement, energitic ions streaming onto the probe surface produce secondary electrons from the surface. The effect of the secondary electrons emission may appreciablly change a probe characteristics from a case in a usual plasma. Secondary electron yield is supposed to be from 2 to 4 for a 10 keV He^+ ion incident upon a tungsten probe and energy distribution of the secondary electrons is assumed to be a maxwellian with a mean energy lower than 10 eV. 13) The probe characteristics under the existence of energitic ions is schematically shown in Fig. 10. The probe current in the ion beam-plasma medium is composed of following four components denoted by (A) to (D). The motion of energitic ions are scarcely affected by the probe potential V_p lower than 100 V in absolute value. Hence a constant

current due to fast ions flows (A). The probe current due to the secondary electrons produced by fast ion impact is constant for $V_p < V_s$ and decays for $V_p > V_s$ according to the energy distribution (B). The current due to cold ions flows for $V_p < V_s$ (C). Upon these currents, usual plasma electron current is superposed (D). A resultant probe current (E) has apparently a large ion saturation current. Typical examples of real probe characteristics are shown in Fig. 11. From the above consideration, we can obtain the informations about electron density n_e, electron temperature T_e and plasma space potential V_s by a usual treatment for a single probe from the probe characteristics in the region $V_p < V_s$, which is convex downward.

A cylindrical probe of tungsten with 1.2 mm in diameter and 6 mm in length was set at the position of 20 cm in front of the target. During the measurement of parameters of the synthesized plasma, the ion source and lens system are typically operated under the condition; (with notations described in Fig. 4) V_{ac}=10 kV, V_2=7 kV, V_3=1 kV, I_d=3 A, I_m=1 A and P_o=0.15 Torr. In Fig. 11, we show probe characteristics for various heating currents of the neutralizer. Ion-and electron-saturation currents increase with the electron emission from the neutralizer. The beam profiles

in the drift chamber for the various heating currents are shown in Fig. 12, which were measured by ion saturation current of the Langmuir probe biased to -100 V. It is noticed again that the electron emission from the neutralizer increases the beam current. In order to check whether the increase of the beam current by electron emission from the neutralizer is brought about due to the suppression of beam expansion caused by ion self space charge, we estimate the radial electric field by ion space charge. Assuming that the radial concentration of beam ions is Gaussian and there is no electron, space potential is determined by Poisson's equation,

$$\frac{1}{r}\frac{d}{dr}\, r\, \frac{d\phi}{dr} = -\frac{n_0 e}{\varepsilon_0} \exp\left(-\frac{r^2}{\sigma^2}\right) ,$$

that is, the maximum radial electric field is given by

$$\left(\frac{d\phi}{dr}\right)_{max} = -\,0.33\, \frac{n_0 e \sigma}{\varepsilon_0} \qquad \text{at} \quad r = 1.12\,\sigma .$$

Using typical parameters $n_0 = 10^8$ cm^{-3} and σ = 5 mm (total ion current amounts to 1.0 mA for 10 keV He^+), the maximum electric field becomes 30 V cm^{-1}. Considering the ion space charge is partially neutralized by the secondary electron from the target, this electric field is not so large for the fast ions to diverge due to the radial force excuted by the radial electric field. This has been confirmed by the facts that

there is no appreciable change in the beam profiles as shown in Fig. 12, and measured radial distribution of the space potential was within some volts independent of the heating power of the neutralizer. We must ask for other origins as a cause of the increase of the beam current. An einzel lens with a retarding potential at the middle electrode slow down accelerated ions. In our case, the retarding potential was needed up to 70% of the extraction potential for sufficient focussing. The retardation of the ions raises the ion density and lengthens the staying time in the region where the axial velocity is small. The retarded ions, therefore, expand radially due to the radial electric field induced by the self space charge. The increase of the beam current caused by heating the neutralizer is explained by the suppression of the beam divergence at the stage of deceleration in the einzel lens system. This is confirmed by examining the effect of the neutralizer for various voltages of V_1 in the configuration of Fig. 5. For sufficiently negative potential of V_1, the beam current becomes insensitive to the heating power of the neutralizer. This neutralization is generally useful for the supperssion of beam divergence occuring in commonly used einzel lens system with retarding potential.

The dependences of the electron temperature T_e, the

space potential V_s and the ion saturation current I_{si} of the probe upon the neutralizer potential V_n are shown in Fig. 13, where the neutralizer was heated sufficiently to emit thermionic electrons. The space potential shown in this figure was determined through a usual data-handling process of probe characteristics. There is, however, a large ambiguity in the determination of space potential. It is difficult to distinguish the existence of a negative a space potential from the existence of an electron stream from a probe characteristics except for an ideal plane probe. 14) Our probe characteristics in case of negative V_n has suggested the existence of two groups of electrons with drifted maxwellian velocity distributions. The two drift velocities are defined by the potential of the neutralizer and the target, respectively. The electron temperature shown in Fig. 13 for $V_n < 0$ is of the component whose drift velocity is determined by the neutralizer potential. It is impossible to determine the electron temperature of the other component with a smaller drift velocity from the probe characteristics because the probe characteristics is smeared by the electron saturation current of the fast component.

Emissivity of the neutralizer lowered appreciably the electron temperature as shown in Fig. 11. This behavior is explained by the fact that sufficient emission of thermionic

electrons neutralizes ion space charge and causes the fall of space potential. The electron temperature was influenced much more by the bias voltage of the neutralizer as shown in Fig. 13. In case of the positive bias, the space potential is determined by the target potential. The target can emit 2 - 3 electrons per incident He ion of 10 keV. These electrons diffuse into the whole drift chamber along the guiding magnetic field. Thermionic electrons from the neutralizer cannot immerse into the plasma becuse of the potential barrier V_n. Thus the electron temperature is mainly determined by secondary electrons emitted from the target. In case of the negative bias, the space potential is a few volt lower than the neutralizer potential. Electrons emitted from the neutralizer can stream into the ambient plasma with mean energy 2 - 3 eV. Secondary electrons from the target cannot immerse into the plasma because of the negative space potential. Hence the electron temperature is mainly determined by the energy distribution of thermionic electrons from the neutralizer. The temperature seems to be determined by the terminal voltage of heating power supply of the neutralizer. As seen from Fig. 13, the electron temperature increases up to 4.5 eV at $V_n=0$ corresponding to the increase of the ion saturation current. Since the energy relaxation time through

collision is estimated to be 500 μ sec for typical plasma parameters; $n=10^8$ cm and $T_e=3$ eV, the temperature rise is not considered due to energy relaxation through classical collisions of both groups of electrons from the target and the neutralizer. The origion of the temperature rise should be asked in the two stream instability between the thermionic electrons from the neutralizer and the fast ions, but the detail could not be clarified.

Energy spectrums of ions in a synthesized plasma is measured with the method described in § 4. All the lens electrode were commonly grounded as in the case without operating the neutralizer in § 3. The bias voltage of the neutralizer was fixed nearly at the ground potential. The energy spread and the most probable energy were insensitive to heating current of the neutralizer and equal to the values in the case without heating the neutralizer. The stability analysis 2) for the longitudinal wave in a synthesized plasma showed that plasma is stable unless the drift velocity of ions is larger than nearly twice the electron thermal velocity. In our typical operating condition the drift velocity of helium ion is 6×10^7 cm/sec at an accelerating voltage 8 kV and nearly half the value of the electron thermal velocity determined by the probe measurement. Therefore the above stability

criterion is satisfied and any collective interaction between the ion beam and neutralizing electrons would not occur.

The dependence of the energy spectrum of ions on the bias voltage of the neutralizer is shown in Fig. 14. When the bias voltage is positive, energy spectrum is insensitive to V_n and is equal to the value at $V_n=0$. When the polarity of the bias voltage is reversed, and lowered down to $V_n= -20$ V, the energy spread amounts to nearly twice the value at $V_n=0$. We have some reasons to state that the streaming ions are scatterd "stochastically" by the fluctuating wave field arising from two stream instability since the presence of streaming electrons with sufficient drift velocity to cause two stream instability is indicated by the probe mesurement. The interpretation is consistent with the behavior of T_e shown in Fig. 13.

By relating the experimental results obtained by the probe measurement with those of the ion energy analysis, it is known that the bias voltage of the neutralizer is most suitable at a few volt negative concerning the beam focussing and energy spread.

6. CONCLUSION

An ion beam extracted from a stationarily operated duoplasmatron was neutralized with thermionic electrons from a hot filament immersed in the beam. The neutralization was effective in suppressing the divergence of the ion beam and increased the beam current measured at a target placed at 100 cm from the ion source. It was confirmed that the neutralization of ion space charge occured mainly under the deceleration electrode of the einzel lens, not in the downstream of the neutralizer. Under the optimum source condition beam current amounted to 8 mA at 15 keV in beam energy and effective beam diameter was about 2 cm. The radial electric field due to ion space charge was very small.

The magnetic field and arc current in the duoplasmatron affected substantially the beam divergence. An increase of the magnetic field and/or arc current brought about the increase of the total beam current extracted from the ion source, but the effective beam current arriving at the target was not necessarily increased. There was an optimum value of the magnetic field and arc current for a given extraction high voltage.

An ion energy analyzing system consisting of an electrostatic deflection analyzer and a pre-decelerator was successfully

employed to measure an energy spread of a few eV among 10 keV in mean energy. The energy spectrum of the extracted ions was substantially affected by the operating condition of the ion source; gas pressure, magnetic field, and arc current. A high plasma density in the arc chamber resulted in a large energy spread. This behavior can be explained by the formation of a potential hill (or a negative anode fall) in front of the anode.

The behavior of thermionic electrons from the neutralizer were affected by the potential of the emitter. A small difference between the space potential and the potential of the emitter changed characteristics of the synthesized plasma, since the drift velocity of thermionic electrons is comparable with the ion drift velocity. From the point of view of beam focussing and energy spread, the bias voltage of the neutralizer was optimum at a few volt negative. Under this condition, the space potential was slightly lower than the bias voltage of the neutralizer and the electron temperature amounted to 3 eV.

In order to produce a synthesized plasma sufficient for utilizing the features with controllable parameters of each components, it is desirable to employ a powerful ion source with higher perviance and a vacuum system with a larger evacuation capacity.

Acknowledgements

The authors wish to express their thanks to prof. K. Takayama, and K. Matsuura and Dr. T. Kuroda for their interest in this work and for their support. The authors are grateful to Dr. S. Fukumoto for valuable advices and comments in designing the ion source and lens system.

This work was performed under the Collaborating Research Program at the Institute of Plasma Physics, Nagoya University, Nagoya.

References

1) J. M. Sellen, Jr., W. Bernstein and R. F. Kemp:
Rev. Sci. Instr. 36, 316 (1965)

2) T. Bolzinger, C. Manus and G. Spiess:
Plasma Physics 11, 411 (1969)

3) M. V. Nezlin:
Plasma physics 10, 337 (1968)

4) E. A. Jackson:
Phys. Fluid 3, 786 (1960)

5) T. E. Stringer:
Plasma Physics 6, 267 (1964)

6) T. Ohnuma and Y. Hatta:
Journal of Phys. Soc. Japan 21, 986 (1966)

7) D. J. Rose and M. Clark, Jr.:
Plasmas and Controlled Fusion (M. I. T. Press, 1961)

8) N. B. Brooks, P. H. Rose, A. B. Wittkower and
R. P. Bastide:
Rev. Sci. Instr. 35, 894 (1964)

9) L. E. Collins, R. H. Fobett and P. T. Stroud:
I. E. E. E. Trans. Nucl. Sci. 12, 247 (1965)

10) G. Gautherin, C. Lejeune, F. Prangere and A. Septier:
Plasma Physics 11, 397 (1969)

11) B. N. Kliarfeld and N. A. Neretina:

Soviet Phys. -Tech. Phys. 28, 271 (1958)

12) A. Septier, F. Prangere, H. Ismail and G. Gautherin:

Nucl. Instr. Meth. 38, 41 (1966)

13) L. Marton ed. :

"Methods of Experimental Physics"

Vol. 4 part A (Academic Press, 1970)

14) S. Ariga:

Journal of Phys. Soc. Japan 31, 1221 (1971)

References

1) J. M. Sellen, Jr., W. Bernstein and R. F. Kemp:
Rev. Sci. Instr. 36, 316 (1965)

2) T. Bolzinger, C. Manus and G. Spiess:
Plasma Physics 11, 411 (1969)

3) M. V. Nezlin:
Plasma physics 10, 337 (1968)

4) E. A. Jackson:
Phys. Fluid 3, 786 (1960)

5) T. E. Stringer:
Plasma Physics 6, 267 (1964)

6) T. Ohnuma and Y. Hatta:
Journal of Phys. Soc. Japan 21, 986 (1966)

7) D. J. Rose and M. Clark, Jr.:
Plasmas and Controlled Fusion (M. I. T. Press, 1961)

8) N. B. Brooks, P. H. Rose, A. B. Wittkower and
R. P. Bastide:
Rev. Sci. Instr. 35, 894 (1964)

9) L. E. Collins, R. H. Fobett and P. T. Stroud:
I. E. E. E. Trans. Nucl. Sci. 12, 247 (1965)

10) G. Gautherin, C. Lejeune, F. Prangere and A. Septier:
Plasma Physics 11, 397 (1969)

11) B. N. Kliarfeld and N. A. Neretina:

Soviet Phys. -Tech. Phys. 28, 271 (1958)

12) A. Septier, F. Prangere, H. Ismail and G. Gautherin:

Nucl. Instr. Meth. 38, 41 (1966)

13) L. Marton ed. :

"Methods of Experimental Physics"

Vol. 4 part A (Academic Press, 1970)

14) S. Ariga:

Journal of Phys. Soc. Japan 31, 1221 (1971)

I_m = 1 A, B_o = 1000 G, V_n = 0, and P_o = 0.15 Torr.

Fig. 12 Radial beam profiles measured by ion saturation current of the Langmuir probe biased negatively to -100 V.

V_{ac} = 10 kV, V_1 = 6 kV, V_{dc} = 1 kV, I_d = 3 A, I_m = 1 A, B_o = 1000 G, V_p = -100 V, V_n = 0, and P_o = 0.15 Torr.

Fig. 13 Variation of plasma space potential, electron temperature and ion saturation current versus bias voltage of the neutralizer. V_{ac}=10 kV, V_1=7 kV, V_{dc}= kV_{ac}=1 kV, I_d=3 A, I_m=1 A, I_n=7.5 A, and B_o=1000 G. The Iens configuration adopted was that shown in Fig. 7.

Fig. 14 Variation of energy spectra half-width versus bias voltage of the neutralizer.

V_{ac} = 5 kV, I_d = 2 A, I_m = 0.7 A, P_o = 0.13 Torr, E_{res} = 90 eV, I_n = 7.5 A, and B_o = 400 G.

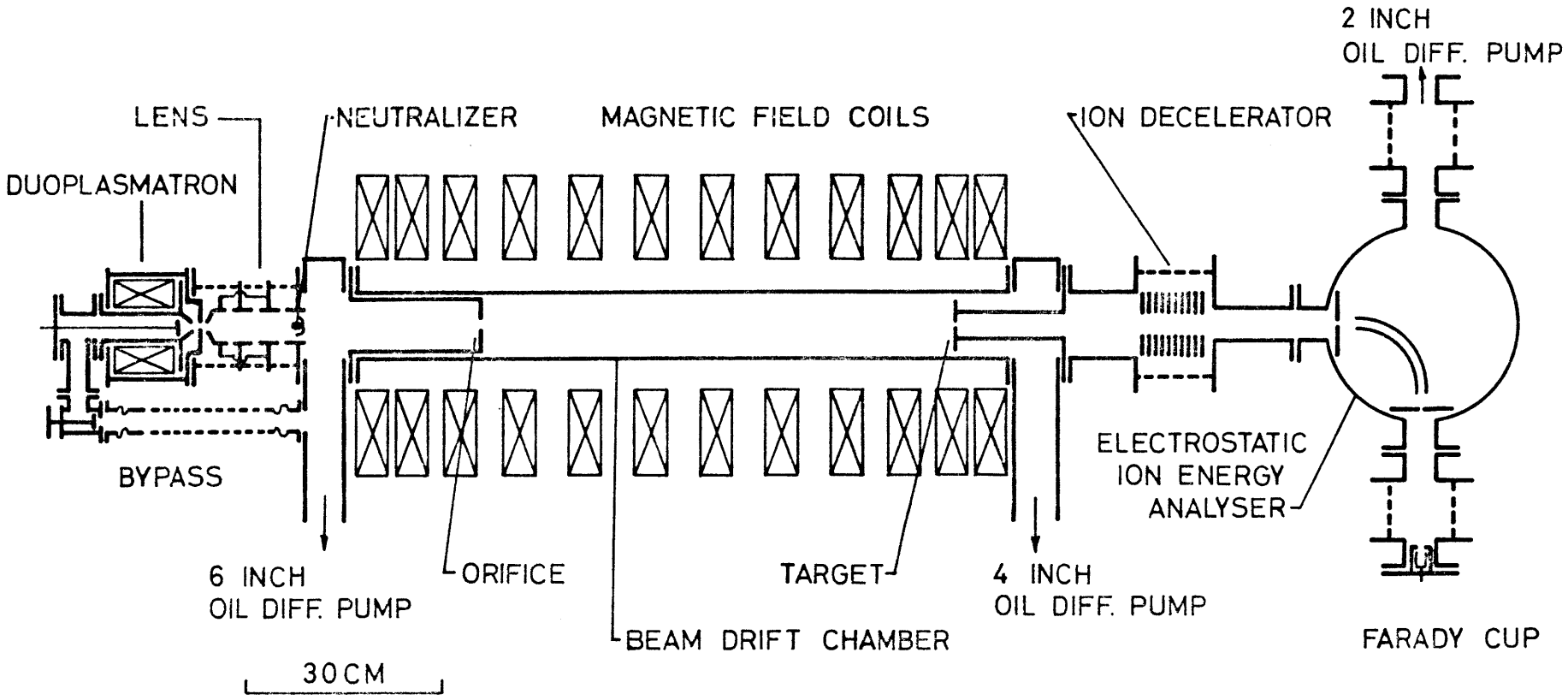
2 INCH
OIL DIFF. PUMP
LENS
NEUTRALIZER
MAGNETIC FIELD COILS
ION DECELERATOR
DUOPLASMATRON
BYPASS
ELECTROSTATIC
ION ENERGY
ANALYSER
6 INCH
OIL DIFF. PUMP
ORIFICE
TARGET
4 INCH
OIL DIFF. PUMP
BEAM DRIFT CHAMBER
FARADY CUP
30CM

Fig.1

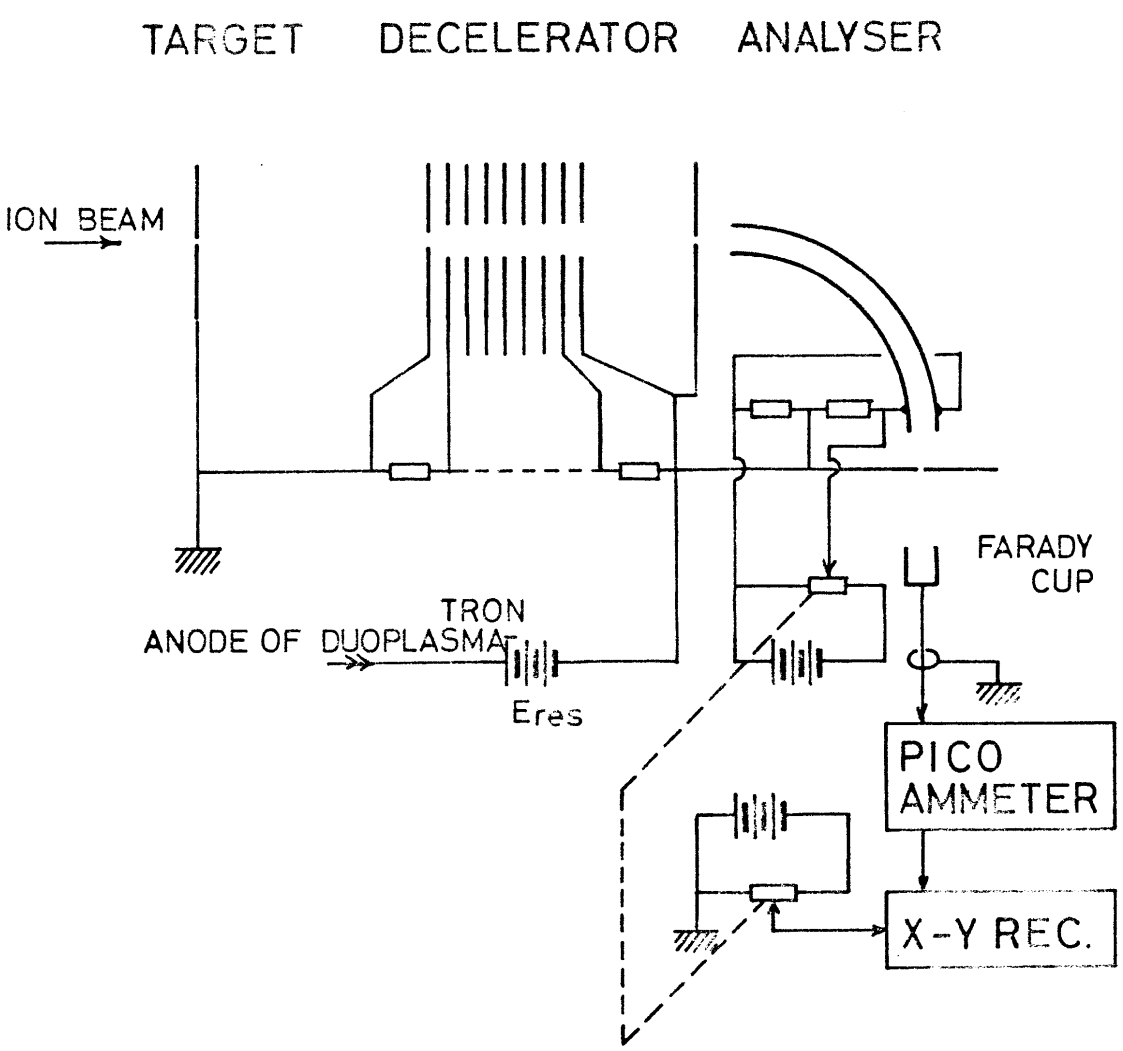
TARGET DECELERATOR ANALYSER
ION BEAM
FARADY CUP
TRON
ANODE OF DUOPLASMAT
Eres
PICO AMMETER
X-Y REC.

Fig.2

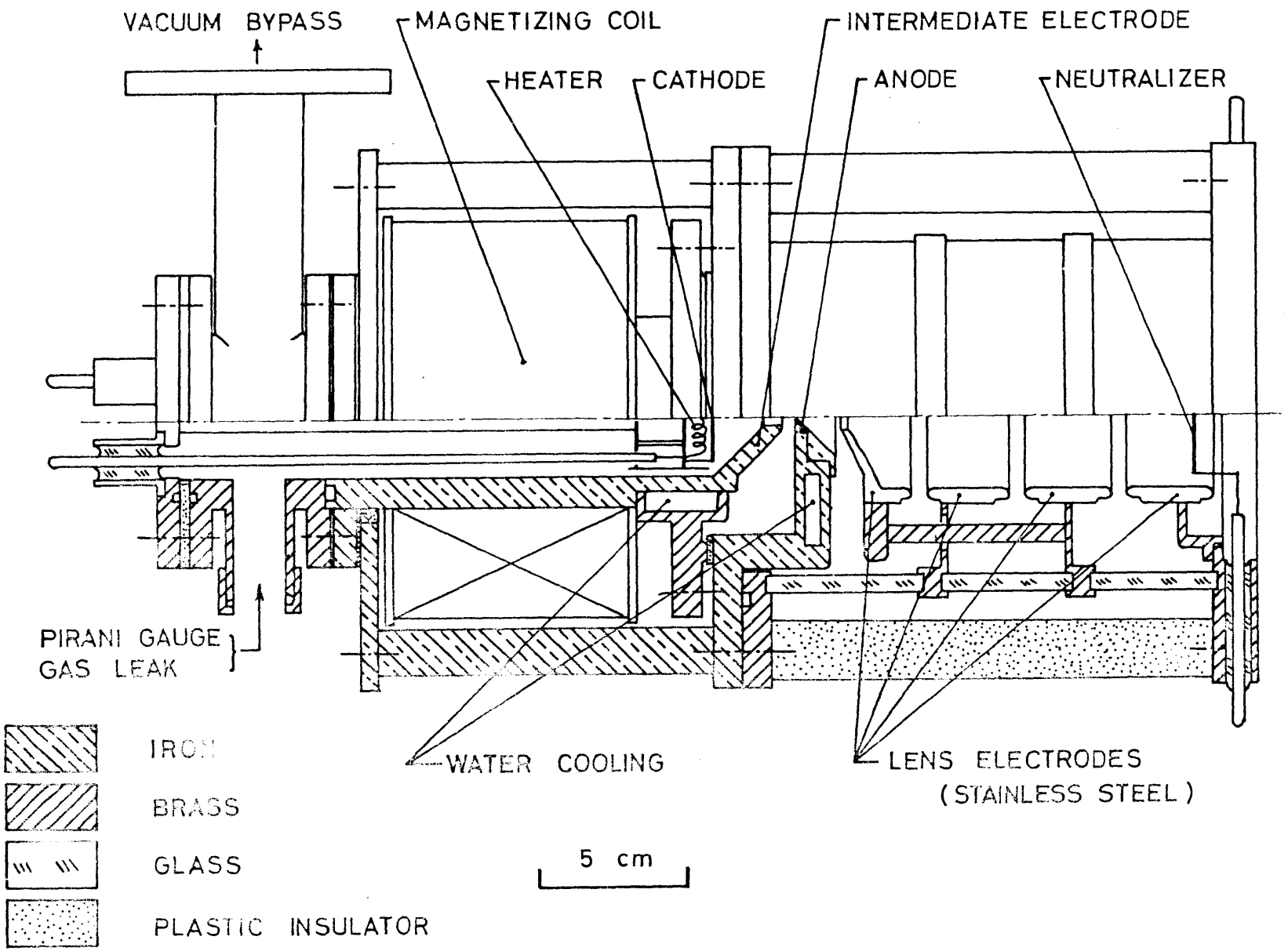
VACUUM BYPASS
MAGNETIZING COIL
INTERMEDIATE ELECTRODE
HEATER
CATHODE
ANODE
NEUTRALIZER
PIRANI GAUGE
GAS LEAK
WATER COOLING
LENS ELECTRODES
(STAINLESS STEEL)
IRON
BRASS
GLASS
PLASTIC INSULATOR
5 cm

Fig.3

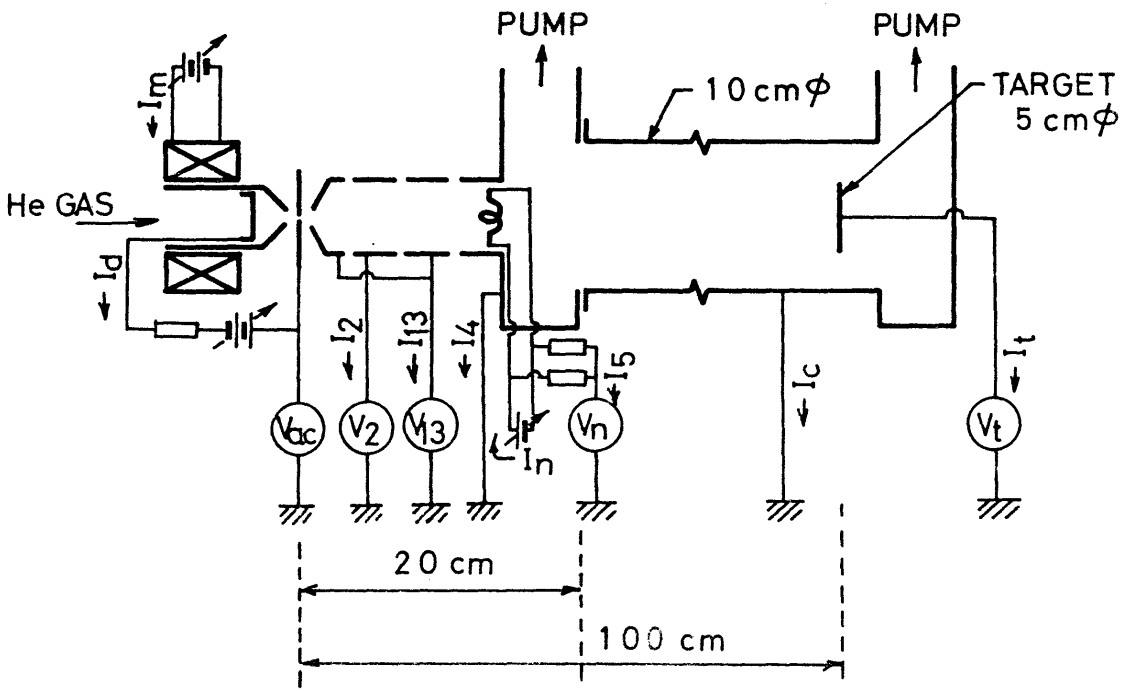
PUMP
PUMP
10 cmφ
TARGET
5 cmφ
He GAS
Im
Id
I2
I13
I4
I5
Ic
It
In
Vac
V2
V13
Vn
Vt
20 cm
100 cm

Fig. 4

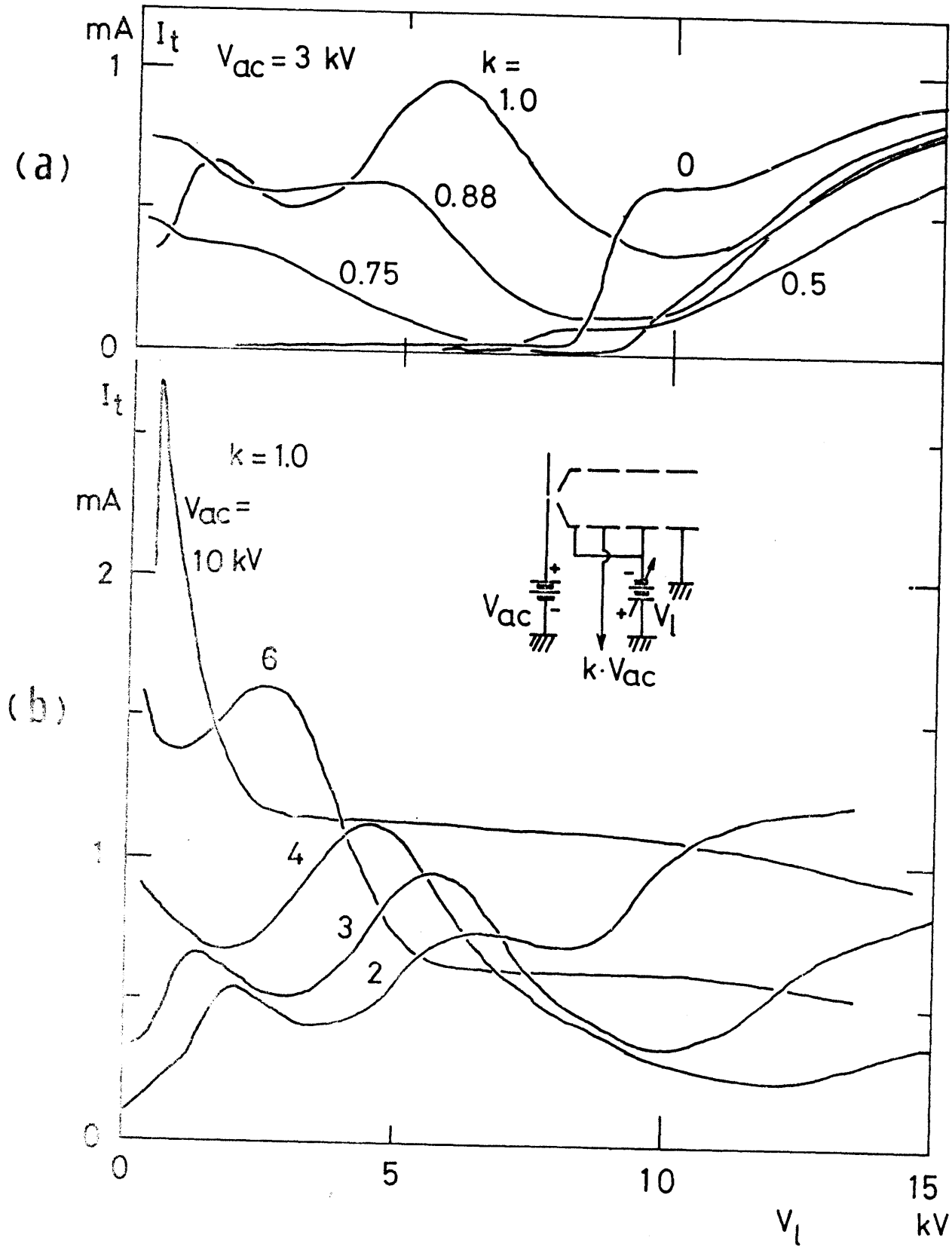
mA
I_t
1
V_{ac} = 3 kV
k =
1.0
0
0.88
0.75
0.5
(a)
I_t
mA
2
k = 1.0
V_{ac} =
10 kV
6
4
3
2
1
0
V_{ac}
V_l
k·V_{ac}
(b)
0
5
10
15
V_l
kV

Fig. 5

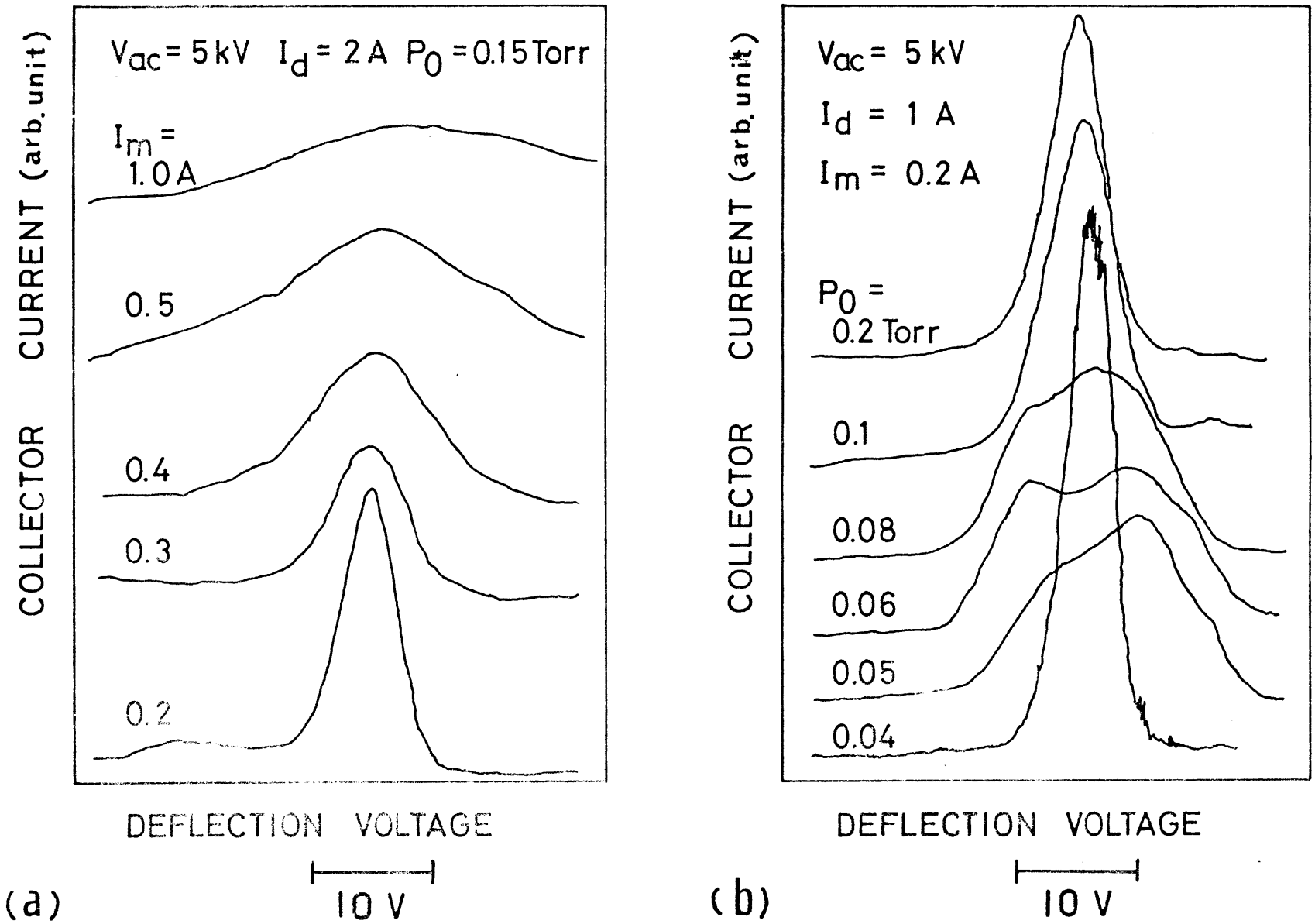
Vac = 5 kV Id = 2 A P0 = 0.15 Torr
Im = 1.0 A
0.5
0.4
0.3
0.2
COLLECTOR CURRENT (arb. unit)
DEFLECTION VOLTAGE
10 V
(a)
Vac = 5 kV
Id = 1 A
Im = 0.2 A
P0 = 0.2 Torr
0.1
0.08
0.06
0.05
0.04
COLLECTOR CURRENT (arb. unit)
DEFLECTION VOLTAGE
10 V
(b)

Fig. 6

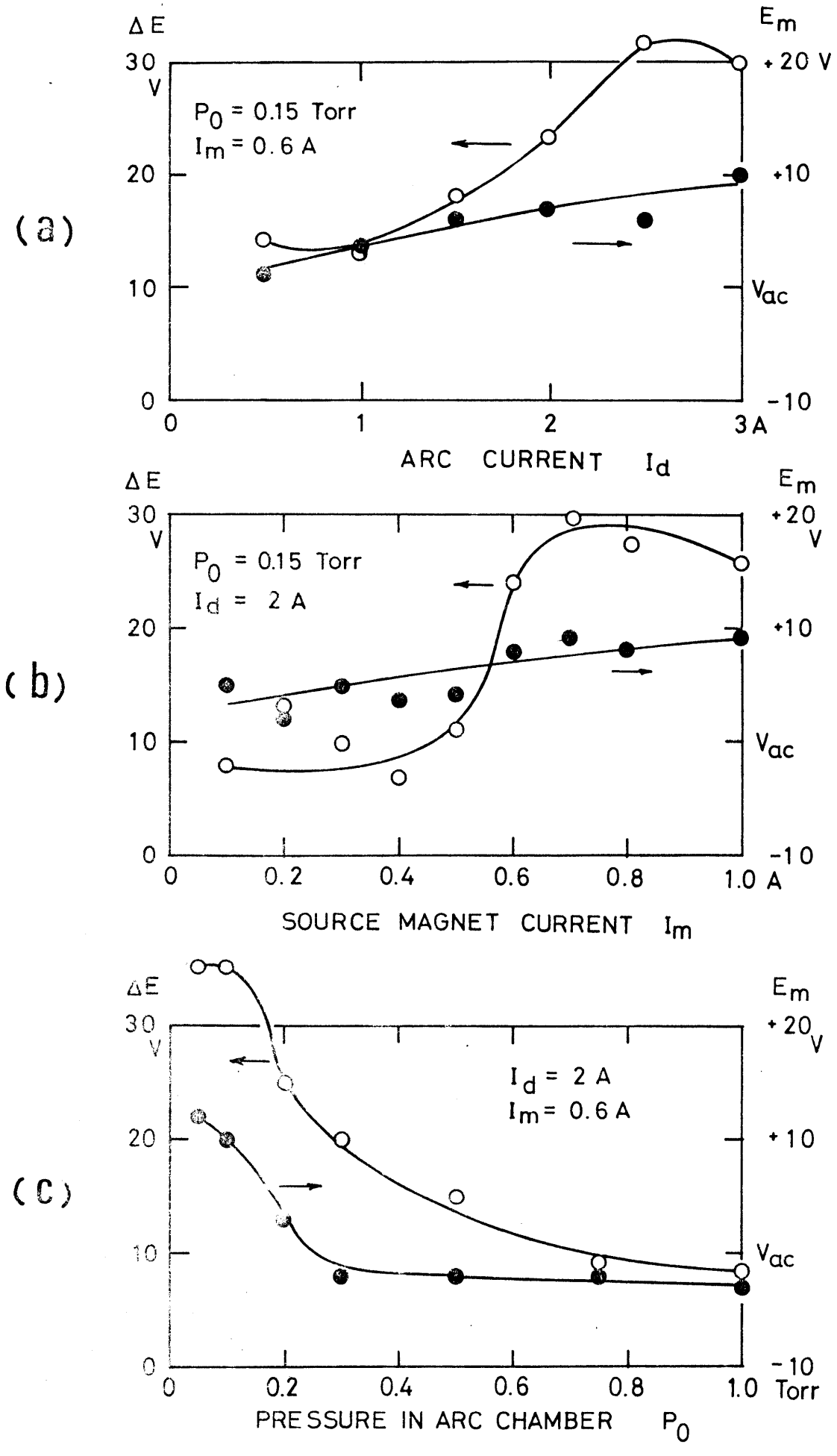
(a)
ΔE
30
V
20
10
0
Em
+20 V
+10
Vac
-10
P0 = 0.15 Torr
Im = 0.6 A
0
1
2
3A
ARC CURRENT Id
(b)
ΔE
30
V
20
10
0
Em
+20
V
+10
Vac
-10
P0 = 0.15 Torr
Id = 2 A
0
0.2
0.4
0.6
0.8
1.0 A
SOURCE MAGNET CURRENT Im
(c)
ΔE
30
V
20
10
0
Em
+20
V
+10
Vac
-10
Id = 2 A
Im = 0.6 A
0
0.2
0.4
0.6
0.8
1.0 Torr
PRESSURE IN ARC CHAMBER P0

Fig. 7

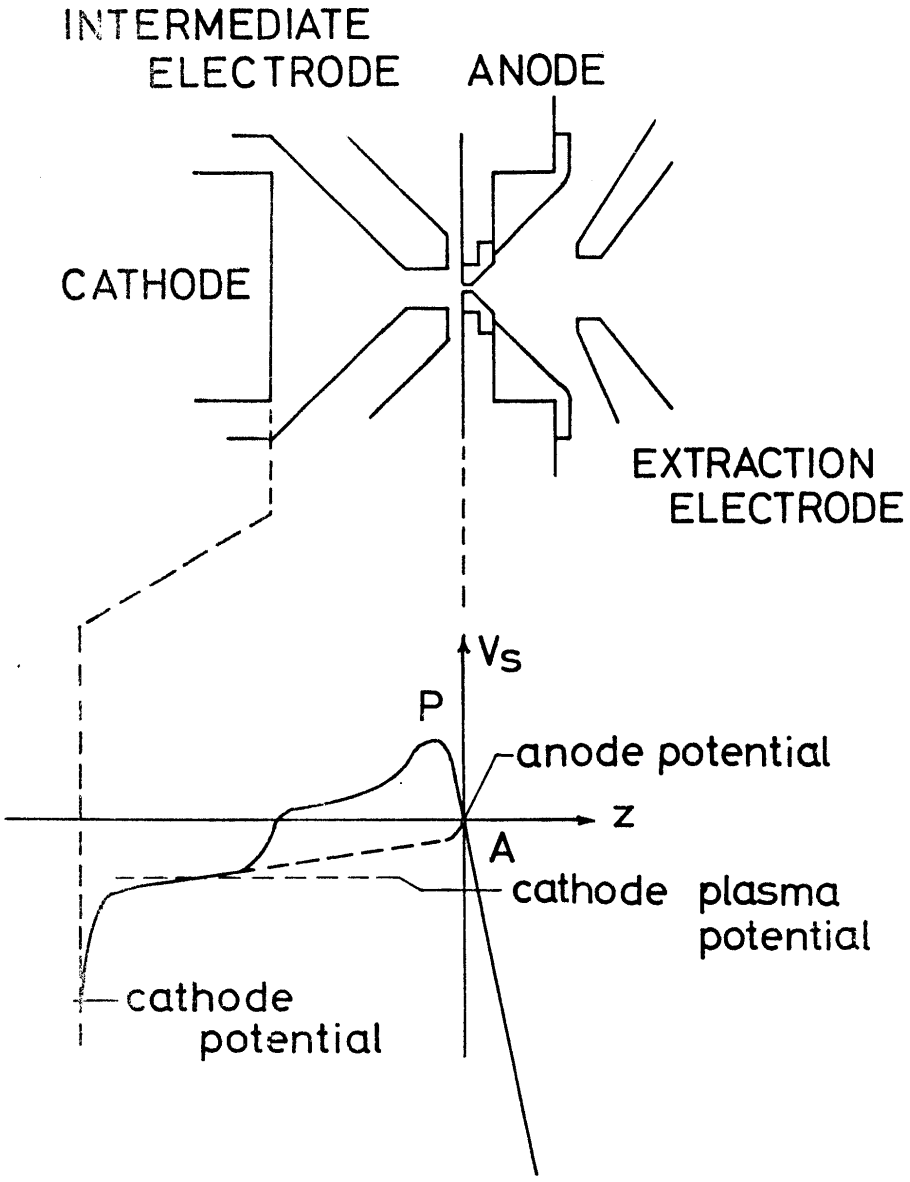
INTERMEDIATE
ELECTRODE
ANODE
CATHODE
EXTRACTION
ELECTRODE
Vs
P
anode potential
z
A
cathode plasma
potential
cathode
potential

Fig. 8

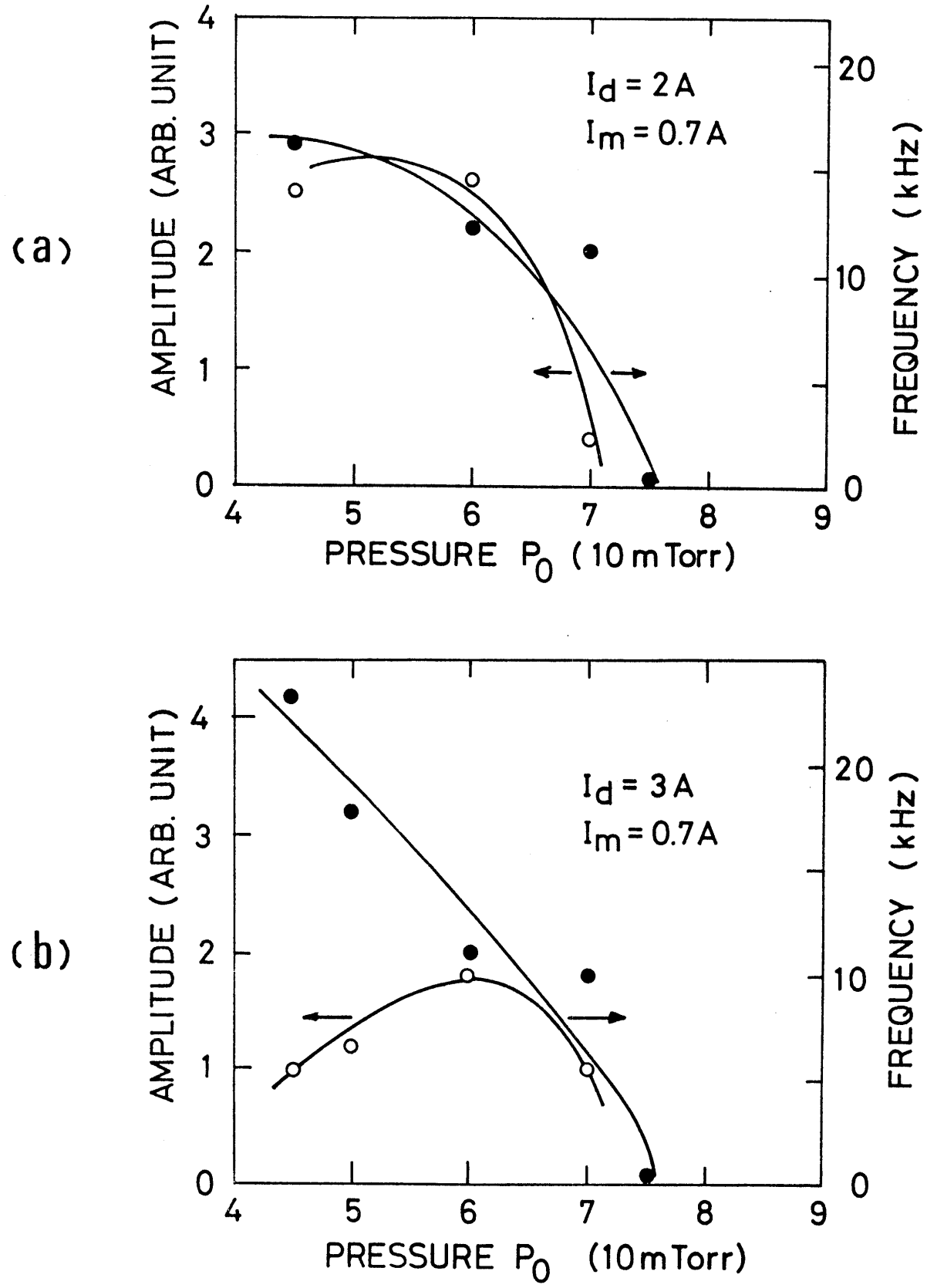
(a)
AMPLITUDE (ARB. UNIT)
FREQUENCY (kHz)
I_d = 2A
I_m = 0.7A
PRESSURE P_0 (10 m Torr)
(b)
AMPLITUDE (ARB. UNIT)
FREQUENCY (kHz)
I_d = 3A
I_m = 0.7A
PRESSURE P_0 (10m Torr)

Fig. 9

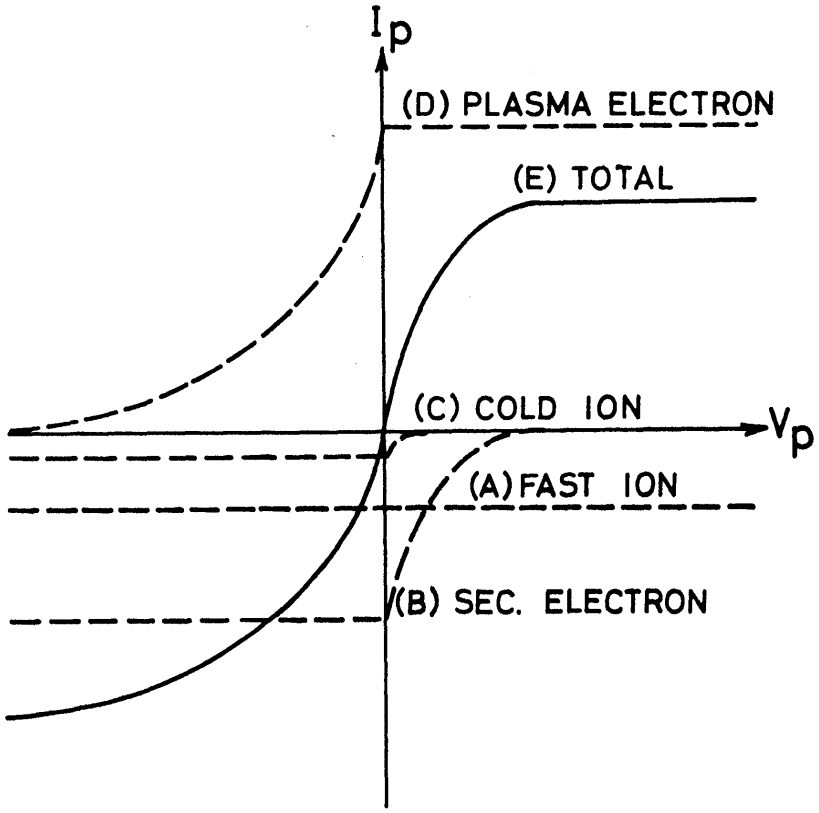
Ip
(D) PLASMA ELECTRON
(E) TOTAL
(C) COLD ION
Vp
(A) FAST ION
(B) SEC. ELECTRON

Fig. 10

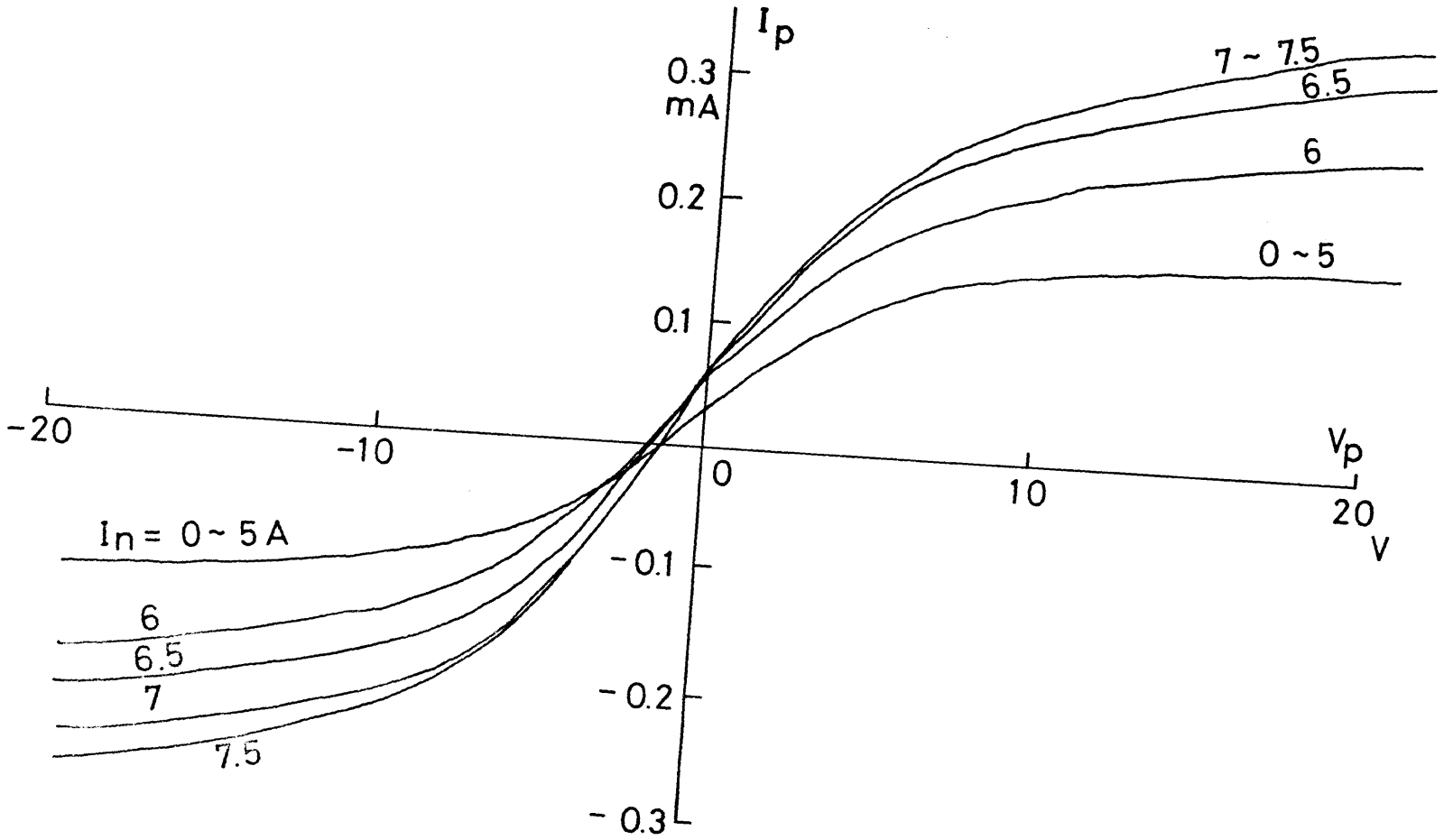

Fig. 11

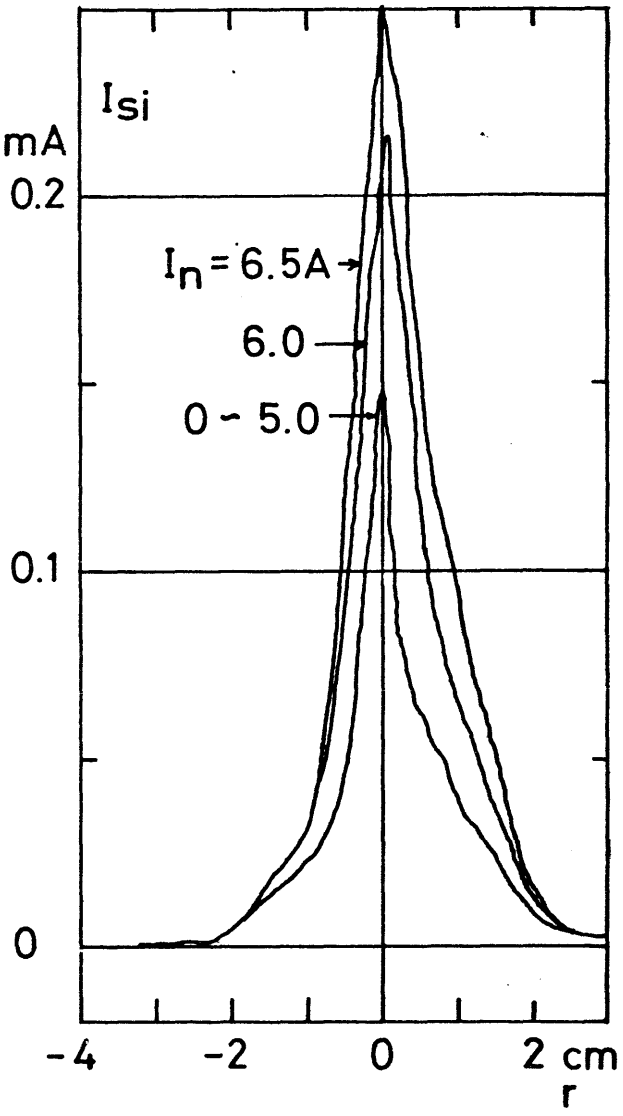

Fig. 12

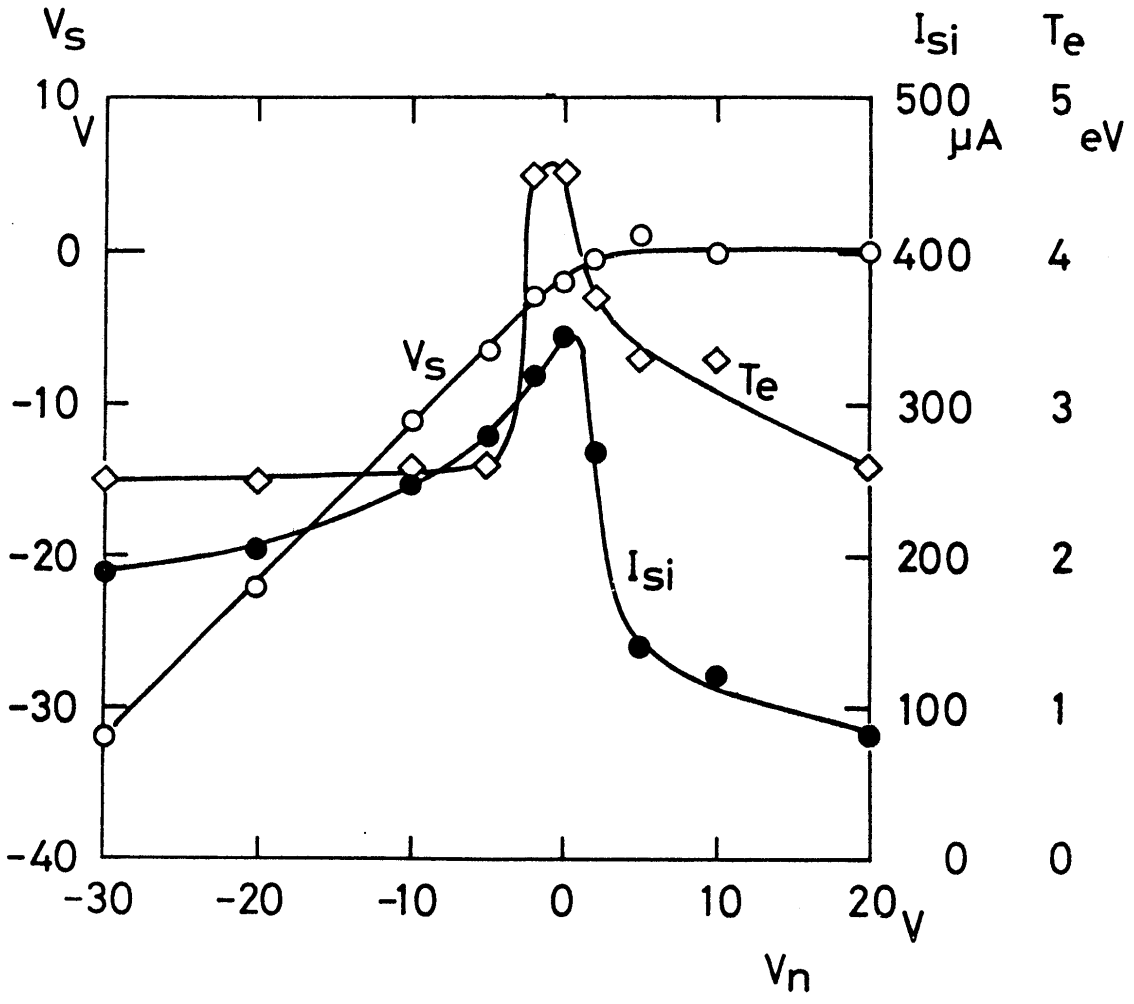
Vs
Isi
Te
10
V
500
μA
5
eV
0
400
4
-10
300
3
-20
200
2
-30
100
1
-40
0
0
-30
-20
-10
0
10
20
V
Vn
Vs
Te
Isi

Fig. 13

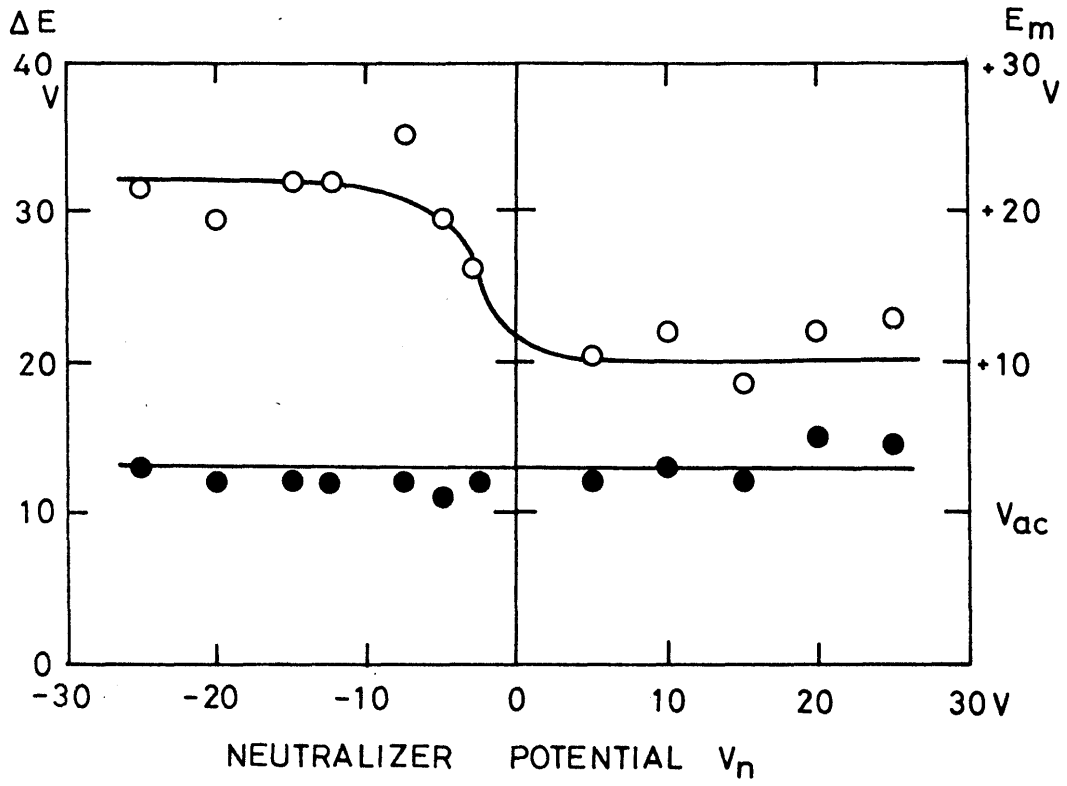
ΔE
40
V
30
20
10
0
-30
-20
-10
0
10
20
30V
Em
+30
V
+20
+10
Vac
NEUTRALIZER POTENTIAL Vn

Fig. 14